

DETERMINATION OF THE TEMPERATURE DISTRIBUTION THE PERFORATED FINS UNDER NATURAL CONVECTION

Dr. Aziz M. Mhamuad
Lecturer
Chemical Eng. Dept.
Technical Institute
Mousl

Thamir Kh. Ibrahim
Assistant Lecturer
Mechanical Eng. Dept
Tikrit University

Raid R. Jasim
Assistant Lecturer

ABSTRACT

This work treats the problem of heat transfer for perforated fins under natural convection. The temperature distribution is examined for an array of rectangular fins (15 fins) with uniform cross-sectional area (100x270 mm) embedded with various vertical body perforations that extend through the fin thickness. The patterns of perforations include 18 circular perforations (holes). Experiments were carried out in an experimental facility that was specifically design and constructed for this purpose. The heat transfer rate and the coefficient of heat transfer increases with perforation diameter increased.

KEYWORDS: Perforated Fins, Temperature Distribution, Natural Convection.

Nomenclature					
symbol	Definition	unit			
k	thermal conductivity of fin material	w/ ^o C m	N_x	Number of perforations in longitudinal direction of the fin	
L	Fin length	m	N_y	Number of perforations in ll direction of the fin	
Nu	Nusselt number of the fin surface	-	OA	Open area of perforated surface	m^2
N_c	Total number of perforations in the fin				

OA_{max}	Maximum open area of perforated surface	m^2	T	Temperature	$^{\circ}C$
Q_f	Heat dissipation rate from the non-perforated fin	W	T_b	Temperature of the fin base	$^{\circ}C$
$Q_{f,max}$	Heat dissipation rate from the non-perforated fin	W	T_a	Ambient temperature	$^{\circ}C$
RAF	Ratio of heat transfer surface area of the perforated fin to that of the non-perforated fin	-	W	Fin width	m
REF	Ratio of the perforated fin efficiency to that of the non-perforated fin	-	η_f	Efficiency of the non-perforated fin	-
REP	Ratio of the perforated fin effectiveness to that of the non-perforated fin	-	η_{fp}	Efficiency of the perforated fin	-
RWF	Ratio of weight of the perforated fin to that of the non-perforated fin	-	ϵ_f	Effectiveness of the non-perforated fin	-
S_x	Longitudinal spacing of the perforation	m	ϵ_{fp}	Effectiveness of the perforated fin	-
S_y	Transverse spacing of the perforation	m	ρ	Density of the fin material	kg/m^3
.t	Fin thickness	m			

INTRODUCTION

One of the basic objectives in design heat exchanger surfaces for enhanced heat transfer is to breakup or disrupts thick laminar boundary layers. Usually this is accomplished by introducing obstructions into the flow or by forming channels which cause local changes in the mean flow direction.

Heat transfer from extended surfaces for a given fin material, base temperature, and ambient temperature can be enhanced by increasing the heat transfer coefficient and / or by increasing the effective heat transfer surface area^[1].

Heat transfer coefficient of the fin surface can be increased by introducing surface roughness and hence promoting turbulence. As for surface area, the literature introduces several methods used to increase the effective heat transfer surface area of fins such as ^[2,3,4]:

- 1-The use of fins comprising rough surface.
- 2-The use of grooved and serrated fins.
- 3-The use of louvered fins.
- 4-The use of slotted and perforated fins.
- 5-The use of augmented fins.

Perforated fins are widely used in plate-fin heat exchangers , film cooling turbine blades , and most recently in a new type of solar collectors used to heat ambient air ^[1,5]

Perforated fins can be used to increase the heat transfer coefficient and /or effective heat transfer area. The change in magnitude of the surface area depends on the geometry of the perforations^[3].

Pin fins, cross-cut fins and augmented fin are examples of the innovations produced by various manufacturers. They all have one thing in common: the improved heat removal

surface has many shorter fin sections that introduce thinner boundary layers than one long fin of the same overall length. Augmented fin allow a lower temperature rise for an equal amount of heat load ^[6]. This fin's is now used in cooling some internal combustion engines; especially the engine which uses in generated the electrical power unit. This fin's now are used in cooling internal combustion engines, specially the engines which uses in generated the electrical power, which are cooling by natural convection.

PREVIOUS WORKS

A series of studies have been conducted for determining the performance of perforated and augmentation heat transfer surfaces:

Liang and Yang^[7] examined the effects of perforation geometry on the heat transfer and friction loss performance of compact heat exchangers having plate perforated rectangular fin surface.

Yang^[8] identified three distinct types of augmentation in the heat transfer and friction loss performance: transition turbulent flow enhancement on low porosity surface, laminar flow

enhancement on high porosity surface, and the entire laminar flow region on low porosity composite surfaces consisting of a short upstream section for producing vortices and a mean section for heat transfer.

Patankar & Prakash^[3] presented an analysis for the flow and heat transfer in an interrupted – plate passage, which is an idealization of the offset fin heat exchanger. The plates are considered to be of finite thickness.

Mullisen & Loehrke^[9] tested arrays of parallel plates in a wind tunnel to identify the important parameters and provide guidelines for designer of heat transfer surfaces and to workers attempting to correlate experimental data. Three distinctly different flow regimes were found within cores composed of in-line plates. These are classified as steady, general unsteady, and periodic unsteady flows.

Fujii et.al^[10] studied experimentally the mechanism of heat transfer enhancement by changing the surface geometries and heat exchanger configuration. The surface has many perforations and is bent to form a trapezoidal shape. Dimensionless

correlations on the heat transfer and pressure drop were presented.

Mousa^[2] examined theoretically the thermal performance for a horizontal rectangular fin with uniform cross-sectional area embedded with four vertical body perforation patterns that extend through the fin thickness. The patterns include circular, square, triangular, and rectangular perforations. Natural convection with finite element technique was used to solve these patterns in his study. The study showed that heat transfer of the perforated fin is larger than that of the non-perforated fin.

MATHEMATICAL TREATMENT

Heat transfer analysis of the non-perforated rectangular fin is based on the analytical solution, based on the following assumptions:

1. The heat conduction in the fin is steady.
2. No heat generation in the fin body.
3. Fin conductivity is constant.
4. The ambient temperature is uniform.
5. The temperature at the base of the fin is uniform.

6. Fin width (w) \gg its thickness (t), so the effect of the fin sides can be neglected.
7. The heat transfer coefficient assumed to be uniform over all surface of the fin.
8. No radiation between the fin and the surrounding.

Based upon these assumptions, the temperature distribution along the non-perforated fin is^[1]:

$$\frac{T_x - T_\infty}{T_b - T_\infty} = \frac{\cosh[m(L-x)] + [h/(mk)]\sinh[m(L-x)]}{\cosh(mL) + [h/(mk)]\sinh(mL)} \dots\dots\dots(1)$$

and heat dissipation rate:

$$Q_f = kA_m(T_b - T_\infty) \frac{\sinh(mL) + [h/(mk)]\cosh(mL)}{\cosh(mL) + [h/(mk)]\sinh(mL)} \dots\dots\dots(2)$$

Where

$$m = \sqrt{\frac{h_t P_f}{kA}}, \quad P_f = \text{peripheral}$$

perimeter = $2W$, A = cross sectional area = $W \cdot t$

The fin performance can be evaluated by the fin efficiency (η_f) or by the fin effectiveness (ε_f). The fin efficiency is defined as the ratio of the heat transfer from the fin to the heat transfer from the fin if its whole body is maintained at the base

temperature. The fin effectiveness is defined as the ratio of the heat transfer rate to the heat transfer rate that would exist without the fin^[1].

$$\eta_f = \frac{Q_f}{Q_{f,max}} \dots\dots\dots(3)$$

$$\varepsilon_f = \frac{Q_f}{h \cdot A_b (T_b - T_\infty)} \dots\dots\dots(4)$$

$$Q_{f,max} = (2LW \cdot h + A_b h)(T_b - T_\infty) \dots\dots\dots(5)$$

Also we can define the heat transfer volume (V), and surface area (A_s) as:

$$V = L \cdot W \cdot t \dots\dots\dots(6)$$

$$A_s = 2LW + W \cdot t \dots\dots\dots(7)$$

GEOMETRICAL ANALYSIS OF FIN PERFORATED

In this paper, the dimensions of fin are known. Also the number of perforations (N_x) in the x- direction (L) and (N_y) in the y- direction (W) can be assumed. The perforation cross sectional area (A_c) may be assumed, and then the dimension of any perforation can be calculated.

The surface area of the uniform longitudinal rectangular perforated fin can be expressed as:

$$\begin{aligned}
 A_{fp} &= A_{ps} + A_t + N_c A_{pc} \\
 &= (2W.L - 2N_c.A_c) + (W.t) + (N_c.A_c) \\
 &= A_f + N_c(A_{pc} - 2A_c) \dots \dots \dots (8)
 \end{aligned}$$

Equation (8) can be written as :

$$A_{fp} = A_f + N_x.N_y(A_{pc} - 2A_c) \dots \dots (9)$$

In order to compare the heat transfer surface area of the perforated fin (A_{fp}) to that of the conventional one (A_f), the fin surface area ratio RAF is introduced and is given by:

$$\begin{aligned}
 RAF &= \frac{A_{fp}}{A_f} \\
 RAF &= 1 + \frac{N_x \times N_y (A_{pc} - 2A_c)}{A_f} \dots (10)
 \end{aligned}$$

The material volume of the perforated fin is compared with the volume of non-perforated fin by volume reduction ratio which given by:

$$\begin{aligned}
 RVF &= \frac{V_{fp}}{V_f} = \frac{(L.W.t - N_x.N_y.A_c.t)}{L.W.t} \\
 RVF &= 1 - \frac{N_x.N_y.A_c}{L.W} \dots \dots \dots (11)
 \end{aligned}$$

Similarly, perforated fin has less weight than that of equivalent non-perforated one. This aspect is

expressed by the fin weight reduction ratio RWF defined as follows:

$$RWF = \frac{W_{fp}}{W_f} = \frac{(W_f - N_x.N_y.A_c.t.\rho)}{W_f}$$

$$RWF = 1 - \frac{(N_x.N_y.A_c.t.\rho)}{L.W.t.\rho} = 1 - \frac{N_x.N_y.A_c}{L.W} \dots \dots \dots (12)$$

According to the perforation shape and dimension that can be cut out from the fin body, fin with the circular perforation pattern is studied. The number of perforation in longitudinal direction (N_x), in the transverse direction (N_y), and the perforation diameter is (b). The directional perforations spacing S_x and S_y :

$$\begin{aligned}
 L &= N_x.b + (N_x + 1)S_y \\
 S_x &= \frac{L - N_x.b}{N_x + 1} \dots \dots \dots (13)
 \end{aligned}$$

$$\begin{aligned}
 W &= N_y.b + (N_y + 1)S_y \\
 S_y &= \frac{W - N_y.b}{N_y + 1} \dots \dots \dots (14)
 \end{aligned}$$

The heat transfer surface area of the fin can be expressed as:

$$A_{fp} = A_f - 2N_c.A_c + N_c.A_p$$

$$\begin{aligned}
 &= A_f + N_c(A_p - 2A_c) \\
 &= A_f + \pi N_c \cdot b \left(t - \frac{b}{2} \right) \dots\dots (15)
 \end{aligned}$$

The ratio RAF and RVF can be expressed as:

$$RAF = 1 + \frac{\pi \cdot b \cdot N_x \cdot N_y \left(t - \frac{b}{2} \right)}{(2W \cdot L + Wt)} \dots\dots(16)$$

and

$$RVF = 1 - \frac{N_x \cdot N_y \cdot \frac{\pi}{4} \cdot b^2}{LW} \dots\dots (17)$$

ANALYSIS OF HEAT TRANSFER COEFFICIENT

An experimental correlation to estimate the convection heat transfer coefficient of array of vertical oriented parallel flat plate is given by^[11]

$$Nu = \frac{h \cdot B}{k} = \frac{Ra}{24} \left(1 - e^{-\frac{35}{Ra}} \right)^{0.75} \dots\dots (18)$$

Where

B is the average space between adjacent fins.

$$Ra = \frac{\rho^2 \cdot g \cdot \beta \cdot C_p \cdot B^4 \cdot \Delta T}{\mu \cdot k \cdot L} \dots\dots (19)$$

Several studies^[9,12,13] reported that the surface heat transfer coefficient

of perforated surfaces is a function of open area ratio [ROA] of the perforated surface . The open area ratio is defined as:

$$ROA = \frac{OA}{OA_{max}} \dots\dots\dots (20)$$

Where OA is the actual open area = $A_c \cdot N_c$

$$= A_c \cdot N_x \cdot N_y \dots\dots\dots(21)$$

OA_{max} is the maximum possible perforations open area, which is defined as:

$$OA_{max} = A_c \cdot N_{c,max} = A_c \cdot N_{x,max} \cdot N_{y,max} \dots\dots(22)$$

where $N_{x,max}$ and $N_{y,max}$ are the maximum possible number of the perforations along the fin. These numbers related with the perforation

spacing equal zero. The perforated surface heat transfer coefficient ratio can be expressed as^[12]:

$$R_h = 1 + 0.75 \frac{OA}{OA_{max}} \dots\dots\dots (23)$$

The film heat transfer coefficient of the perforated surface (h_{ps}) is expressed as:

$$h_{ps} = (1 + 0.75 \frac{OA}{OA_{max}})h \dots\dots\dots (24)$$

EXPERIMENTAL WORK

The experiments were carried out in an experimental facility that was specifically designed and constructed for this purpose. Figure (1) shows view of the experimental apparatus.

The experimental setup includes a heat sink supplied with heating elements and data acquisition system,. The heat is generated within the heat sink by means of four heating elements each of 650 W powers. All the experimental data are recorded by the data acquisition system.

The components of the system used to carry out the experiments are given below:

Heat Sink Assembly

The heat sink chosen for experiments Fig.(2) is aluminum cylinder of 100 mm diameter and 270 mm length. Four holes were drilled in the cylinder in which four heating elements were pressed. The power supplied by each element was 650 W. Fifteen aluminum straight fins were

fitted radially. The fins are 100 mm long, 270 mm wide and 2 mm thick. These fins were divided into five groups equally :

A-non-perforated fins.

1. perforated fins with 8mm diameter perforation.
2. perforated fins with 12mm diameter perforation.
3. perforated fins with 16mm diameter perforation.
4. perforated fins with 20mm diameter perforation.

All groups include three fins and we taken the middle of them as a test fin.

Power Supply Regulator

A variable transformer Fig(1) of type 50B with input 220V and 50-60Hz and output 0-240V, 20A, and 7.5kVA was used to regulate the voltage supplied to the heating elements.

The measurement

The experimental data were measured by thirty calibrated thermocouples of type-K were used to measure the temperature at different locations necessary for this study. The measured parameters and their ranges during the experiments were listed below:

- Heat supplied: 100-900 W.
- Perforation-shape: Circular.
- Number of perforation: 18 per fin with various diameter of perforation.

The temperatures of testing fins were measured by using thirty thermocouples of type-k. Three of these thermocouples fixed on the outside diameter of the aluminum cylinder in order to measure the base temperature of the fin. Two thermocouple are used to measure air temperature.

Twenty five of thermocouples were divided into five groups equally (the same number of fin groups). Each group was fixed to the surface of the test fin at equal space (20 mm) locations along the fin length.

The apparatus was allowed to run for about 100 minute, until the steady state was attained. The recording of temperature was started after steady state had been reached.

RESULTS AND DISCUSSION

Equation (8) for the investigated perforation shape geometry indicate that the increase or decrease in surface area of the perforated fin, with respect to that of the non-perforated one, depends on the following parameters: the total

number of perforation (N_c), the perforation diameter(b),and the fin thickness.

However, the above Equation also imply that A_{fp} is greater or smaller than A_f depending on the fin thickness (t) and perforation diameter (b).

Equation (10) shows that the heat transfer surface area of the perforated fin is a function of the fin dimensions and the perforation shape geometry. This Equation can be used to calculate the ratio of the heat transfer surface area of the perforated fin to that of the non-perforated one, RAF. It indicates that RAF is a weak function of the fin length and width. This is because the effect of the fin tip area which is smaller compared surface to that of the fin surface area and can be neglected.

Figure (3) express the relation between RAF and perforation diameter (b). This figure shows that (RAF) is smaller than unity.

Heat dissipation rate of the perforated fin depends on the heat transfer coefficient and fin area. In this study, all the film heat transfer coefficients are assumed to be uniform and equal. It was mentioned before that (R_h) s always greater than unity and

increasing up to the upper limit 1.75 as the diameter (b) increased, but decreasing down to the lower limit of 1. The calculation of heat transfer coefficient ratio R_h (Equation 23) was plotted in Figure (4).

The temperature distribution along the fin has important effect on the fin performance. Higher fin temperatures exist as the fin thermal resistance is decreased. The temperature distribution of the perforated fins and that non-perforated along x -direction are plotted in Figures (5) through (13). As shown in figures, it is obvious that the temperatures along the non-perforated fin are higher than those of the perforated one in most cases. These figures indicate that the temperature drop between the fin base and tip increases as the perforation diameter increased. This is because the thermal resistance of the perforated fin decreases as the perforation diameter is increased.

The perforated fin weight reduction ratio (RWF) for the perforated fin type can be calculated from Equation (12). The ratio RWF is plotted as a function of the perforation diameter (b) in Figure (14). The figure shows that the weight reduction ratio of the perforated

fin continues to decrease as b is increased.

CONCLUSIONS

The rate of temperature drop along the perforated fin length is consistently larger than that for the equivalent non-perforated fin. The gain in heat dissipation rate for the perforated fin is a strong function of both: the perforation dimension and lateral spacing. Decreasing the perforation dimension reduces the rate of temperature drop along the perforated fin. Heat transfer coefficient for perforated fin is larger than of non-perforated one.

REFERENCES

1. Incropera, P. and Dewitt, D.P., "Fundamentals of heat and mass transfer", 5th Edition, John Wiley and Sons, 2001.
2. Mousa, A.H., "Enhancement of thermal performance of fins subjected to natural convection through body perforation", Ph.D. thesis, Mech. Eng., Baghdad university, 2000.
3. Patankar, S.V., and Prakash, C., "An analysis of the effect of plate thickness on laminar flow and heat transfer in

- interrupted plate passage", Int.J.H .T, Vol.29, No.11, 1981.
4. Zelenk, R.L., and Loehrke, R.I., "Heat transfer from interrupted plates", J. of H.T., Vol.105, 1983.
 5. Jarrah, B.A., "Thermal optimization of pin fin arrays experiencing forced convection heat transfer", M.Sc. Thesis, Jordon, 1996,
 6. Mhamud, A.A., "Performance of perforated and non-perforated fins", Ph.D. Thesis, Chemical Eng., University of Baghdad, 2005.
 7. Liang, C.Y. and Yang, W.J., "Heat transfer and friction loss performance of perforated heat exchanger surfaces", J. of H.T., Feb. 1975.
 8. Yang., W.J., "Three kinds of heat transfer augmentation in perforated surfaces", Letters in H. and M.T., Vol.5, 1978.
 9. Mullisen, R.S., and Loehrke, R.I., "A steady of flow mechanism responsible for heat transfer enhancement in interrupted-plate heat exchangers", J. of H.T., Vol.108, 1986.
 10. Fujii, M. et.al., "Heat transfer and pressure drop of perforated surface heat exchanger with passage enlargement and contraction", Int.J.H.M.T., Vol.31, No.1, 1988.
 11. Simmons R.E. ., "Estimation natural convection heat transfer for arrays of vertical parallel flat platter " Electronics cooling, Feb. 2002
 12. Kakaee,S., "Heat exchanger thermal-hydraulic fundamentals ", 1989.
 13. Rohsenow, W.M., Hartnett, J.P., and Ganic, E.N., "Handbook of heat transfer fundamentals", 2nd Edition, McGrew-Hill Book company, 1982.

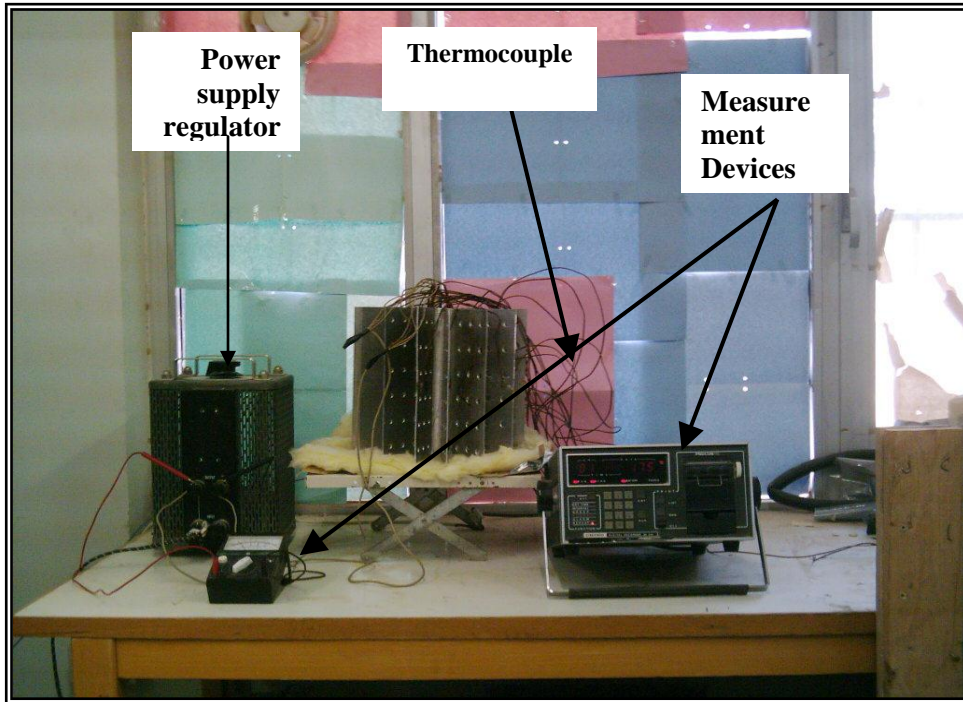
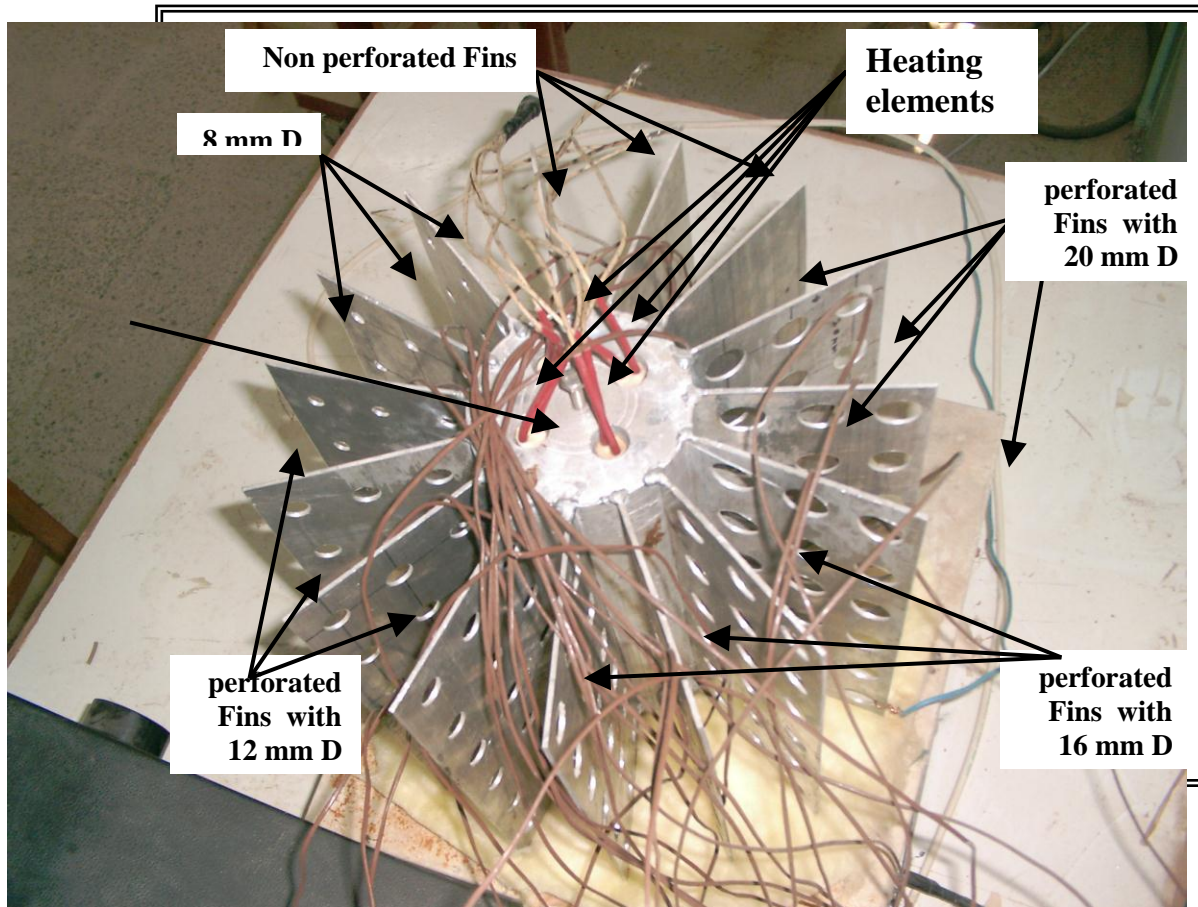


Figure (1) View of the Experimental Apparatus



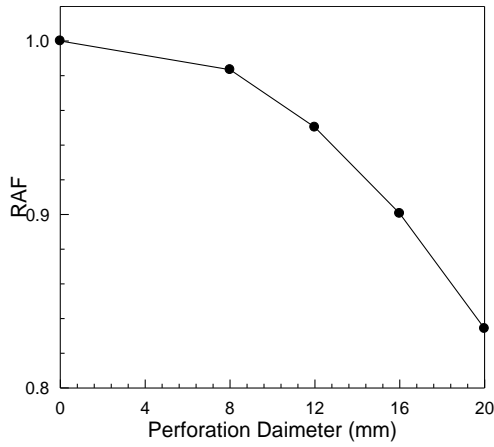


Figure (3) the relation between ratio of heat transfer surface area of perforated fin to that of non perforated fin RAF and perforation diameter.

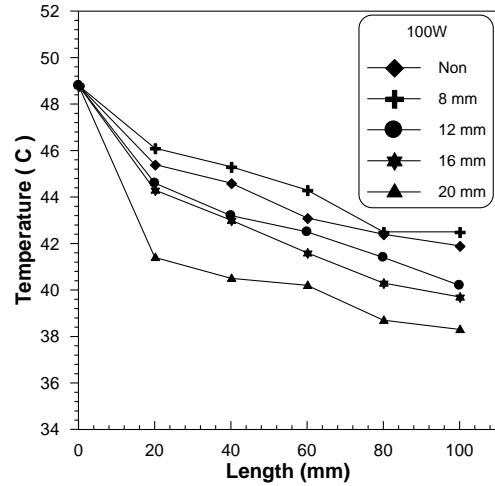


Figure (5) Temperature Distribution with 100w

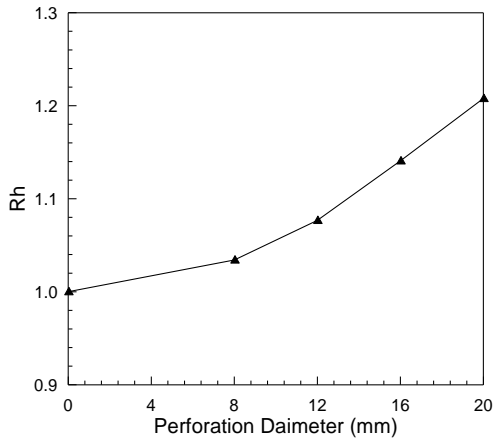


Figure (4) The relation between heat transfer coefficient ratio (Rh) and perforation diameter.

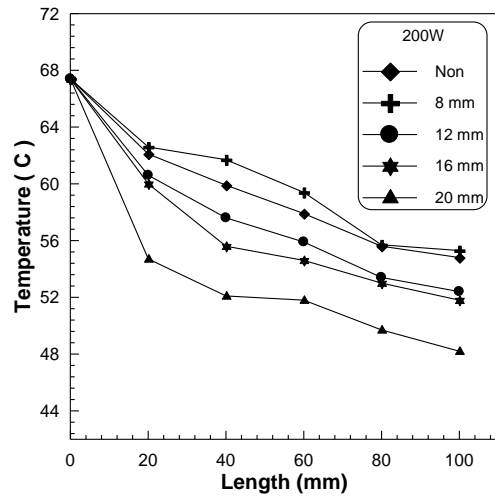


Figure (6) Temperature Distribution with 200w

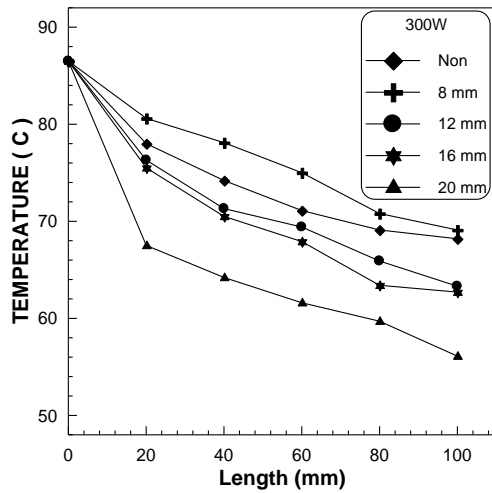


Figure (7) Temperature Distribution with 300w

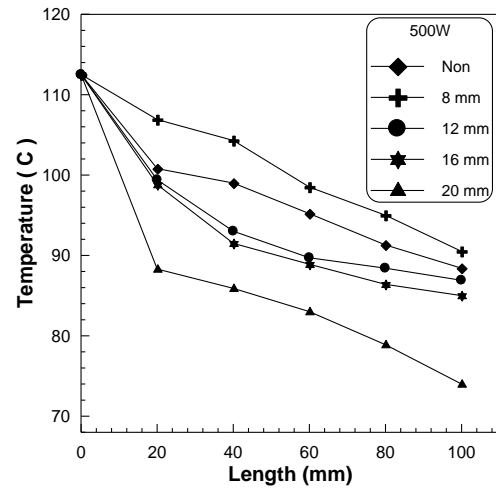


Figure (9) Temperature Distribution with 500w

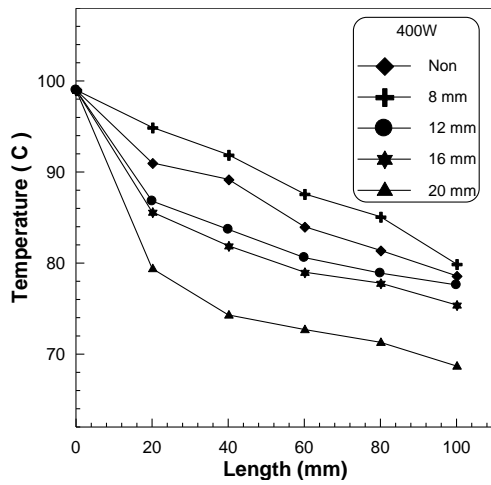


Figure (8) Temperature Distribution with 400w

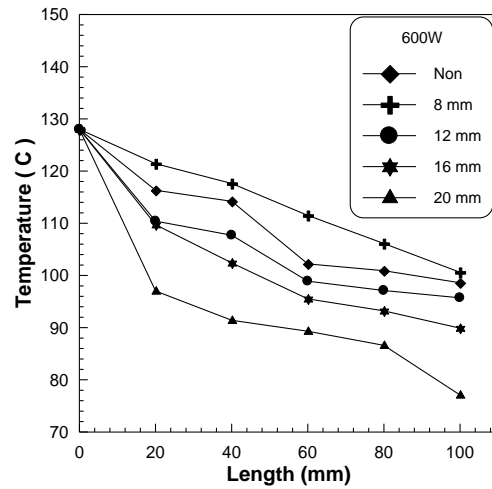


Figure (10) Temperature Distribution with 600w

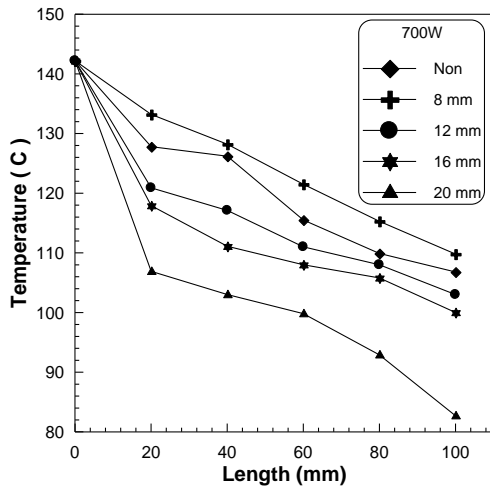


Figure (11) Temperature Distribution with 700w

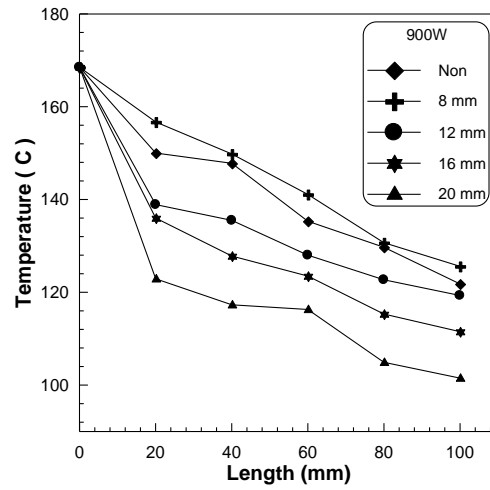


Figure (13) Temperature Distribution with 900w

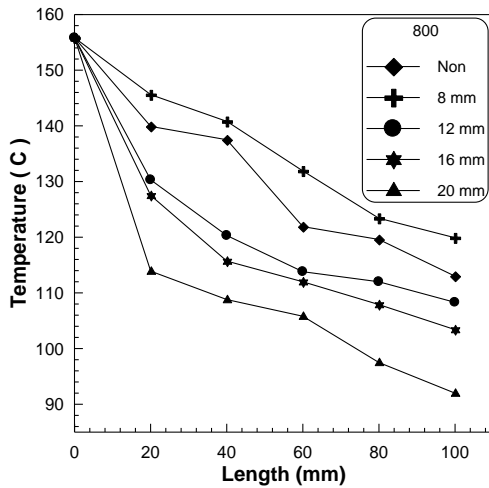


Figure (12) Temperature Distribution with 800w

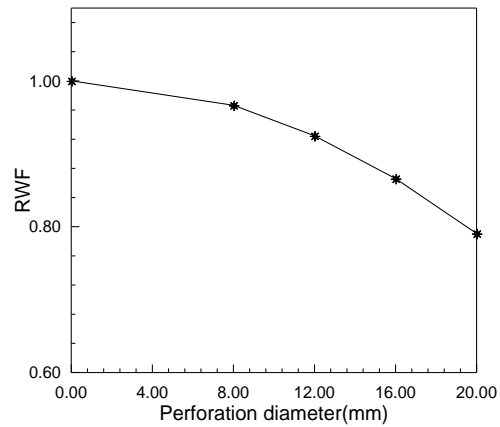


Figure (14) The relation between ratio of weight of perforated fin to that of non perforated fin(RWF) and perforation diameter.

إيجاد توزيع درجات الحرارة في الزعانف المثقبة دائريا تحت تأثير الحمل الطبيعي

رائد رشاد جاسم

ثامر خليل إبراهيم

د.عزيز محمد محمود

مدرس مساعد

مدرس مساعد

مدرس

قسم الهندسة الميكانيكية

المعهد التقني

جامعة تكريت

الموصل

الخلاصة

تهدف الدراسة إلى معالجة انتقال الحرارة من الزعانف الحاوية على ثقوب دائرية تحت تأثير الحمل الطبيعي. تم قياس توزيع درجات الحرارة لمجموعة من الزعانف (15 زعنفة) المستطيلة (270 x 100 ملم) والحاوية على ثقوب دائرية. إن عدد الثقوب في جميع الزعانف متساوي (18 ثقب)، وهي موزعة على ستة أعمدة وثلاثة صفوف. تم تصميم وإنشاء جهاز مختبري خاص لغرض إنجاز هذا البحث. أثبتت الدراسة أن كلا من معدل انتقال الحرارة ومعامل انتقال الحرارة في الزعانف يزدادان بزيادة أقطار الثقوب.

الكلمات الدالة : الزعانف المثقبة ، توزيع درجات الحرارة ، الحمل الطبيعي.